

# An improved implementable process for the synthesis of zeolite 4A from bauxite tailings and its Cr<sup>3+</sup> removal capacity

Peng-cheng Lei, Xian-jiang Shen, Yang Li, Min Guo, and Mei Zhang

School of Metallurgical and Ecological Engineering, University of Science and Technology Beijing, Beijing 100083, China  
(Received: 17 December 2015; revised: 22 January 2016; accepted: 25 January 2016)

**Abstract:** A simple and practical method for the synthesis of zeolite 4A from bauxite tailings is presented in this paper. Systematic investigations were carried out regarding the capacity of zeolite 4A to remove Cr(III) from aqueous solutions with relatively low initial concentrations of Cr(III) (5–100 mg·L<sup>-1</sup>). It is found that the new method is extremely cost-effective and can significantly contribute in decreasing environmental pollution caused by the dumping of bauxite tailings. The Cr(III) removal capacity highly depends on the initial pH value and concentration of Cr(III) in the solution. The maximum removal capacity of Cr(III) was evaluated to be 85.1 mg·g<sup>-1</sup> for zeolite 4A, measured at an initial pH value of 4 and an initial Cr(III) concentration of 5 mg·L<sup>-1</sup>. This approach enables a higher removal capacity at lower concentrations of Cr(III), which is a clear advantage over the chemical precipitation method. The removal mechanism of Cr(III) by zeolite 4A was examined. The results suggest that both ion exchange and the surface adsorption–crystallization reaction are critical steps. These two steps collectively resulted in the high removal capacity of zeolite 4A to remove Cr(III).

**Keywords:** bauxite; tailings; zeolite; trivalent chromium; wastewater treatment

## 1. Introduction

Water pollution is a serious environmental problem that has caused severe shortages of clean drinking water in many parts of the world. Moreover, booming global industrial development has produced a huge quantity of wastewater, which is often discharged directly into rivers or lakes without effective treatment. Wastewater usually contains many toxic and harmful substances such as oil, organics, and heavy metal ions. Chromium usually exists in three valence states, *viz.* bivalent chromium (Cr(II)), trivalent chromium (Cr(III)), and hexavalent chromium (Cr(VI)). Hexavalent chromium is a common toxic heavy metal ion that can cause serious soil and water pollution because of its high toxicity. The toxicity of Cr(VI) is 500 times greater than that of Cr(III). Moreover, Cr(III) may be readily transformed into Cr(VI) under certain conditions such as pH changes and highly oxidative conditions [1–2]. Thus, the containment of Cr(III) discharge in wastewater is a high priority with regard

to providing a sustainable environment for living beings.

Currently, there are many methods for treating wastewater containing chromium, such as chemical precipitation, ion exchange methods, biological methods, electrolytic methods, and photocatalytic methods [3–4]. Among these, chemical precipitation is a traditional water treatment process that has many advantages such as mature technology, low investment cost, low process cost, and a high level of automation; this method has been applied extensively worldwide. However, many studies have achieved only a partial removal of chromium ion from wastewater by this method with the initial concentration of Cr ranging from 100 to 300 mg·L<sup>-1</sup> [5–6]. Consequently, this method cannot effectively remove chromium at low concentrations.

Recently, the use of low-cost sorbents has emerged as a simple and effective technique to remove Cr from water and wastewater. Among the cost-effective materials, zeolites are considered to be applicable in view of their strong adsorption and ion exchange capacities [7–8].

Zeolites are crystalline aluminosilicate materials with an

Corresponding author: Mei Zhang E-mail: zhangmei@ustb.edu.cn

© University of Science and Technology Beijing and Springer-Verlag Berlin Heidelberg 2016

open three-dimensional framework structure. They have regular, uniformly sized, microscopic interconnected pores and windows, which provide access to molecules that are smaller than the zeolites themselves while excluding larger molecules [9–11]. Among the more than 200 different types of zeolites, zeolite 4A is one of the most important, due to its widespread industrial applications. Zeolite 4A has been used in adsorbents [12–14], ion-exchangers [15–16], gas separators [17–19], drug carriers [20], and detergent builders [21–22]. This zeolite has a small pore size of 0.41 nm in diameter, and its molar ratio of Si/Al is about 1. This low Si/Al molar ratio of zeolite 4A correlates well with the large amount of aluminum used to provide exchange sites for balancing cations, which results in enhanced ion-exchange capacity for zeolite 4A [16,23]. Moreover, zeolite 4A has high selectivity for the removal of metal ions, and the exchangeable sodium ions are relatively innocuous. It is reasonable to expect that Cr(III) at a low concentration can be removed by zeolite 4A, in contrast to the shortcomings of the chemical precipitation method. However, the costs of the raw materials are relatively high for zeolite 4A synthesis. With the development of technology, various waste products from certain industries are being explored as ingredients to reduce production costs. In this context, bauxite tailings can be considered as a suitable alternative source.

Bauxite tailings are the waste generated during the beneficiation process to improve the Al/Si molar ratio in bauxite. About 0.2 t of bauxite tailings are generated per ton of bauxite ore after the flotation process [24]. However, only a very small proportion of bauxite tailings are used; a large amount of bauxite tailings are still stored in the tailing dam, which can be harmful to the environment and can endanger public health. With the continuous draining of resources on earth and the increase in the environmental consciousness of human beings, many countries consider tailings to be a secondary resource. Extensive research is being carried out regarding the utilization of bauxite tailings.

In our previous work, zeolite 4A was successfully synthesized from bauxite tailings [25]. However, too much acid and alkali species were used in the synthetic process, which led to a relatively high production cost. Therefore, a simple and cost-effective method to synthesize zeolite 4A from bauxite tailings is provided in the present work.

## 2. Experimental

### 2.1. Synthesis of zeolite 4A

The materials used for the synthesis of zeolite 4A powders were bauxite tailings (Zhengzhou, Henan Province,

China) as the source of Al and some Si, Na<sub>2</sub>SiO<sub>3</sub>·9H<sub>2</sub>O (Sinopharm Chemical Reagent Company, SCRC, analytical pure) as a supplementary Si and Na source, and NaOH (pellets, SCRC, 96wt%) as the fused salt. The synthetic method of zeolite 4A from bauxite tailings was improved on the basis of our previous work reported in Ref. [25]. As shown in Fig. 1, after a series of treatments, including alkali fusion, dissolution in water, filtering, gel synthesis, crystallization, filtration, washing, and drying, bauxite tailings were transformed into zeolite 4A.

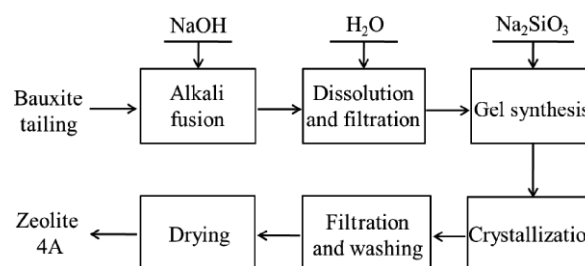


Fig. 1. Flow sheet of zeolite 4A synthesized from bauxite tailings.

Compared with the previous method, the acid leaching process was eliminated, and a hydrothermal method was used to synthesize zeolite 4A from a gel in the crystallizing process. First, bauxite tailings and sodium hydroxide were mixed in a mass ratio of 1:1, placed in a graphite crucible and calcined in a muffle furnace at 500°C for 30 min. Second, a mixture of 5 g of the calcined product and 60 mL of deionized water in a beaker was maintained at 25°C for 15 min under stirring (300 r/min). Third, the solution was separated from the mixture by a filtration process. The molar ratio of Na<sub>2</sub>O:Al<sub>2</sub>O<sub>3</sub>:SiO<sub>2</sub> in the solution was adjusted to 4.29:1:1.9 by the addition of 4.86 g of Na<sub>2</sub>SiO<sub>3</sub>·9H<sub>2</sub>O. Subsequently, the solution was stirred (500 r/min) for 30 min at room temperature and then placed in a hydrothermal synthesis reactor to synthesize zeolite 4A. The hydrothermal synthesis reactor was maintained in an electrothermal constant-temperature box at 95°C for 5 h after which the zeolite 4A sample could be obtained following the filtering, washing, and drying steps. The calcium ion exchange capacity of the zeolite 4A was measured and compared with that reported in the literature [25].

### 2.2. Removal of Cr(III) by zeolite 4A

In order to investigate the removal efficiency of Cr(III) by zeolite 4A, a Cr(III) stock solution was firstly prepared. 0.77 g of Cr(NO<sub>3</sub>)<sub>3</sub>·9H<sub>2</sub>O (AR) was dissolved in 1 L of deionized water, and the concentration of Cr(III) in the stock solution was maintained at 100 mg·L<sup>-1</sup>. The process of re-

removal of Cr(III) by zeolite 4A was as follows. A given mass of zeolite 4A was directly added to the Cr(III) solution at a designated initial concentration and pH value in a 250 mL beaker; the mixtures were then allowed to react at 25°C for 4 h with continuous stirring at 500 r/min; finally, after 4 h of reaction, the mixture was filtered and the concentration of Cr(III) remaining in the solution was measured. The removal efficiency for Cr(III) ions was calculated using the following equation:

$$\text{Removal efficiency} = \frac{c_0 - c_e}{c_0} \times 100\% \quad (1)$$

where  $c_0$  is the initial Cr(III) concentration ( $\text{mg}\cdot\text{L}^{-1}$ ), and  $c_e$  is the final Cr(III) concentration ( $\text{mg}\cdot\text{L}^{-1}$ ).

The removal capacity refers to the amount of Cr(III) removed by unit mass of zeolite 4A. The removal capacity of Cr(III) by zeolite 4A was calculated using the following equation:

$$\text{Removal capacity} = \frac{c_0 - c_e}{m} \times V \quad (2)$$

where  $V$  is the volume of the aqueous phase (L), and  $m$  is the amount of zeolite 4A used (g) [23].

Various factors could affect the removal capacity of Cr(III) by zeolite 4A; the main factors considered were the initial pH value and the initial Cr(III) concentration in the solution. The effects of initial pH value on the removal of Cr(III) by 100 mg zeolite 4A were studied in an aqueous solution with  $100 \text{ mg}\cdot\text{L}^{-1}$  Cr(III) concentration. The initial pH values of the five Cr(III) solutions were adjusted to 3.0, 3.5, 4.0, 4.5, and 5.0, respectively, using  $0.1 \text{ mol}\cdot\text{L}^{-1}$  nitric acid or  $0.1 \text{ mol}\cdot\text{L}^{-1}$  sodium hydroxide solution as modifiers. After reacting for 4 h, the final pH value in each solution was measured with a pH meter. At the same time, a blank experiment was prepared to investigate the effects of chromium chemical precipitation generated as the pH value increased: instead of adding zeolite 4A, sodium hydroxide solution was added to the five solutions to directly adjust their initial pH values to the corresponding final pH values; then the concentration of remaining Cr(III) in the solution was measured in order to calculate the mass of the chromium precipitated.

The effects of the initial concentration of Cr(III) on the removal of Cr(III) by zeolite 4A in solution were investigated in 100 mL solution. The initial concentrations of Cr(III) in the solutions were 100, 50, 25, 10, and  $5 \text{ mg}\cdot\text{L}^{-1}$ . The initial pH value was adjusted to 4.0 with  $0.1 \text{ mol}\cdot\text{L}^{-1}$  nitric acid or  $0.1 \text{ mol}\cdot\text{L}^{-1}$  sodium hydroxide solution. In this process, the mass of zeolite 4A added to the solution was proportional to the mass of Cr(III), namely, 100, 50, 25, 25, and 5 mg, respectively.

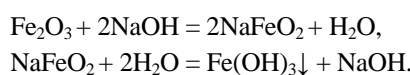
## 2.3. Characterization

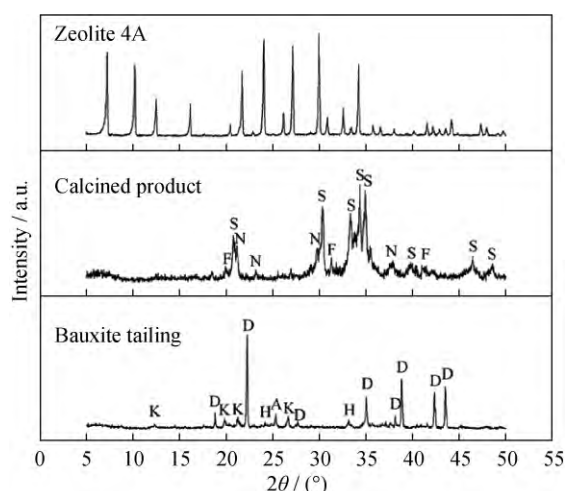
Powder X-ray diffraction patterns of the samples were obtained using a powder diffractometer (TTRIII PW 12 kW) equipped with a Cu  $K_\alpha$  radiation source. The accelerating voltage and current used were 40 kV and 100 mA, respectively. The chemical compositions of the solid powders obtained in each step were measured using an X-ray fluorescence spectrometer (XRF-1800, Japan). The surface morphologies of the specimens were observed using a field emission scanning electron microscope (SEM, Zeiss, Supra-55) coupled with energy dispersive X-ray analysis (EDS). In the SEM analysis, the samples were coated with a thin layer of carbon and mounted on conducting glass. The particle size was measured by laser beam scattering technique (LMS-30). The pH values of the aqueous solutions were measured with a pH meter (PHS-25C). All the concentrations of Cr(III) in the solution were detected by the 1,5-diphenylcarbazide analysis method [23–24].

## 3. Results and discussion

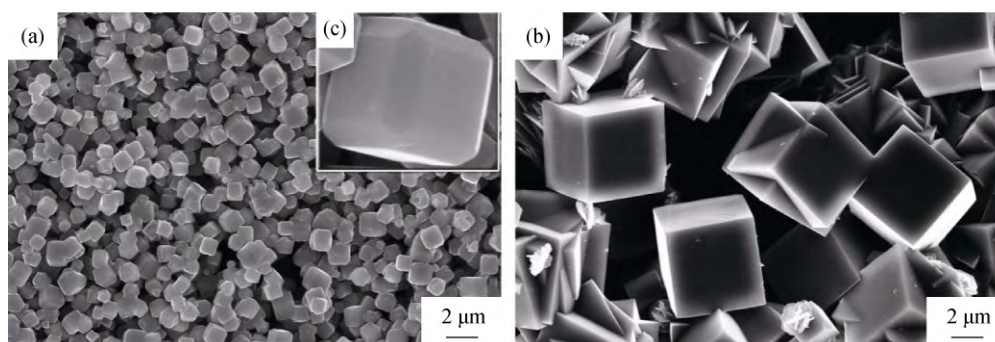
### 3.1. Synthesis of zeolite 4A from bauxite tailings

Fig. 2 shows the X-ray diffraction (XRD) pattern of the bauxite tailings. It was found that the main crystal phases were diaspore ( $\text{Al}_2\text{O}_3\cdot\text{H}_2\text{O}$ ), kaolinite ( $\text{Al}_2\text{O}_3\cdot 2\text{SiO}_2\cdot 2\text{H}_2\text{O}$ ), hematite ( $\text{Fe}_2\text{O}_3$ ), and anatase ( $\text{TiO}_2$ ). The presence of Fe element could severely affect the synthesis of zeolite 4A from bauxite tailings. Therefore, it was necessary to remove the iron impurity beforehand. In the previous synthetic process, Fe was removed from bauxite tailings by the acid leaching method, while other useful elements (Al, Si) remained in the residue. Chemical equation  $\text{Fe}_2\text{O}_3 + 6\text{HCl} = 2\text{FeCl}_3 + 3\text{H}_2\text{O}$  shows the detailed chemical reaction. However, in contrast to the previous method, in the new synthetic process without acid leaching, Fe was removed from the bauxite tailings by alkali fusion, leaching, and filtering processes. The XRD pattern of the calcined product is presented in Fig. 2. It was found that the main crystal phases were sodium aluminum oxide ( $\text{NaAlO}_2$ ), nepheline ( $\text{NaAlSi}_3\text{O}_8$ ), and sodium iron oxide ( $\text{NaFeO}_2$ ). The presence of  $\text{NaFeO}_2$  indicated that hematite was converted to  $\text{NaFeO}_2$  in the alkali fusion process. It is generally known that  $\text{NaFeO}_2$  is easily hydrolyzed in aqueous solution to yield the precipitate  $\text{Fe}(\text{OH})_3$ , which can be removed in the subsequent filtering process. The detailed chemical reactions are shown as follows:





**Fig. 2.** XRD patterns of the bauxite tailings, the calcined product, and the sample of zeolite 4A synthesized from the bauxite tailings. D, K, H, A, S, N, and F represent diaspore, kaolinite, hematite, anatase, sodium aluminum oxide, nepheline, and sodium iron oxide, respectively.



**Fig. 3.** SEM images of the zeolite 4A samples: (a) and (b) represent the zeolite 4A samples synthesized by the new and previous methods, respectively; (c) represents a partial enlarged view of the crystalline grain in image (a).

A comparison of the present process route to the earlier method designed by the present group highlights that the new method could not only eliminate environmental pollution from the acid leaching process, but also greatly reduce the production cost due to its simplified process and lower alkali charge. This method could also lead to an increase in performance, especially with respect to the calcium exchange capacity. Moreover, compared to the industrial method of using expensive, pure chemical raw materials to synthesize zeolite 4A, the new method of using much less expensive bauxite tailings as the Al source could reduce the production cost by about 30%.

### 3.3. Removal of Cr(III) by zeolite 4A

The effects of the initial pH value and the initial concentration of Cr(III) ions on the removal of Cr(III) were investigated. Also, the removal mechanism of Cr(III) by zeolite 4A is discussed in the subsequent sections.

Fig. 2 also shows the XRD pattern of a sample of zeolite 4A synthesized from bauxite tailings. This sample was identified as single phase zeolite 4A (JCPDS card 39-0222).

### 3.2. Characterization of zeolite 4A samples

Fig. 3 shows SEM images of the samples of zeolite 4A synthesized from bauxite tailings by the new and previous methods. The mean diameters of the samples of zeolite 4A synthesized by the two methods were 1 to 2  $\mu\text{m}$  and 6 to 14  $\mu\text{m}$ , respectively. Fig. 3(c) shows that the morphology of the zeolite 4A sample synthesized by the new method was a chamfering cubic shape, which is very different from that of the sample prepared by the earlier method.

In the present work, the calcium exchange capacity (expressed in terms of  $\text{CaCO}_3$ ) of the zeolite 4A sample synthesized by the new method was measured and was found to be  $328 \text{ mg}\cdot\text{g}^{-1}$ , which was much higher than the previous value of  $296 \text{ mg}\cdot\text{g}^{-1}$ .

#### 3.3.1. Effect of initial pH value on the removal of Cr(III) by zeolite 4A

Considering two facts that the solid insoluble species Cr(III) would be formed when the pH value of the solution is greater than 6 and that zeolite 4A would be dissolved when the pH value of the solution is less than 2, the initial pH value was limited to the range of 3–5 [26–28]. Fig. 4 shows the removal efficiency for Cr(III) ions over this pH range in a fixed zeolite 4A mass of 100 mg at an initial Cr(III) concentration of  $100 \text{ mg}\cdot\text{L}^{-1}$  in the solution.

As can be seen in Fig. 4, the Cr(III) removal efficiency of zeolite 4A was dependent on the pH value. When the pH value was increased from 3 to 4, the Cr(III) removal efficiency of zeolite 4A increased from 26.8% to 45.1%. This was partly due to the effect of competition between Cr(III) and  $\text{H}_3\text{O}^+$  for the bonding sites in the crystalline grains of the zeolite 4A sample [21,29]. At lower pH values, an excess of  $\text{H}_3\text{O}^+$  could compete effectively with Cr(III) for the

bonding sites, resulting in a lower level of Cr(III) absorption on the zeolite 4A. In contrast, when the pH value was further increased to 5, the Cr(III) removal efficiency of zeolite 4A resulted in a decrease from 45.1% to 25.7%. This was attributed to the fact that a major portion of Cr(III) could transform into Cr(OH)<sub>3</sub> and precipitate at a relatively higher pH value, which leads to a reduction of the removal efficiency of Cr(III) by zeolite 4A. From the blank experimental tests, at the initial pH range of 3 to 4, the removal of Cr(III) due to Cr(OH)<sub>3</sub> precipitation was less than 10%, which would not significantly affect the removal efficiency of Cr(III) by zeolite 4A. However, at an initial pH value of 5, the precipitation dramatically increased to 50%, which would seriously affect the removal efficiency of Cr(III) of the zeolite 4A sample. Therefore, in the experiments that followed, the initial pH value of the solution was fixed at 4.

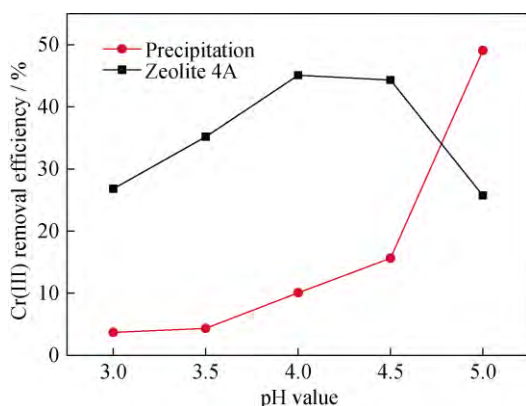


**Fig. 4.** Pure removal efficiency of Cr(III) by zeolite 4A sample (black line) or by precipitation (red line) at different initial pH values (temperature, 25°C; time, 4 h; volume, 100 mL; mass of zeolite 4A, 100 mg; Cr(III) initial concentration, 100 mg·L<sup>-1</sup>).

### 3.3.2. Effect of initial Cr(III) concentration on the removal of Cr(III) by zeolite 4A

In order to investigate the influence of the initial Cr(III) concentration on the Cr(III) removal capacity of zeolite 4A, a comparative study with five different Cr(III) concentrations was carried out at an initial pH value of 4 in the solution; the results are shown in Fig. 5.

It could be seen that the Cr(III) removal capacity gradually increased from 45.1 mg·g<sup>-1</sup> to 85.1 mg·g<sup>-1</sup> with decreasing Cr(III) concentration. This clearly indicates that much more Cr(III) would be removed per unit mass of zeolite 4A at lower initial concentrations of Cr(III) in the solution. Further, these results also indicated that the higher removal capacity of Cr(III) by zeolite 4A at lower concentrations of Cr(III) in the solution could overcome the drawbacks of the chemical precipitation method.

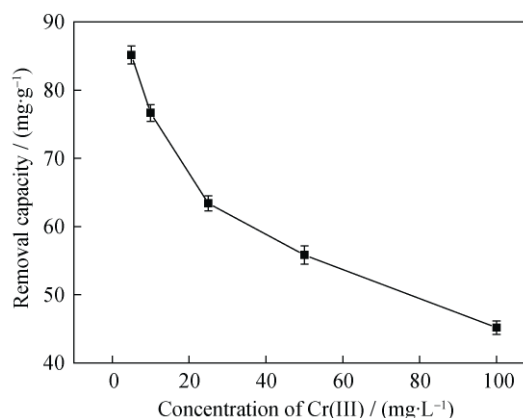


**Fig. 5.** Removal capacity of Cr(III) by the zeolite 4A sample at different concentrations of Cr(III) in the solution (temperature, 25°C; time, 4 h; volume, 100 mL; pH 4).

### 3.3.3. Effect of zeolite 4A dose on the removal of Cr(III)

To investigate whether the concentration of Cr(III) remaining in the solution after the removal reaction would be lower than that required by the national demand, excess zeolite was added to the solution to improve the removal efficiency of Cr(III). Fig. 6 shows the removal efficiencies of Cr(III) at a concentration of 5 mg·L<sup>-1</sup> in different doses (the ratio of the mass of zeolite 4A added to the solution to the volume of the solution). As can be observed from Fig. 6, the removal efficiency of Cr(III) gradually increased with increasing dose of zeolite 4A and reached 96.8% at the dose of 0.150 g·L<sup>-1</sup>. This was due to the increase of the available surface area per unit volume of solution with the increasing dose of zeolite 4A. However, the removal efficiency did not show any noticeable increase when the dose of zeolite 4A sample was more than 0.125 g·L<sup>-1</sup>. This would mean that a small amount of Cr(III) always remained in the solution. A small amount of Cr(III) that had been absorbed on the zeolite 4A could be redissolved into the solution due to the existence of hydrolytic equilibrium. However, under the conditions of the maximum removal efficiency, the concentration of Cr(III) remaining in the solution after removal reaction was 0.16 mg·L<sup>-1</sup>, which is far below the emission standard of Cr(III) in industrial sewage (<0.5 mg·L<sup>-1</sup>). These results illustrated that the zeolite 4A synthesized from bauxite tailings could effectively remove Cr(III) from aqueous solution.

### 3.3.4. Effect of time on removal of Cr(III) by zeolite 4A

In order to investigate the effect of time on the removal of Cr(III) by zeolite 4A, a kinetic study was carried out in the solution with an initial Cr(III) concentration of 100 mg·L<sup>-1</sup> and an initial pH value of 4; the results are shown in Fig. 7. It was observed that the Cr(III) removal efficiency increased rapidly during the first 30 min and subsequently

became stable, with a slight scatter. This indicated that the Cr(III) removal efficiency could reach about 47% in 30 min.

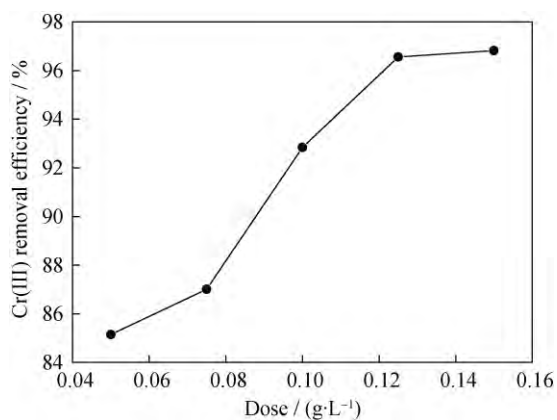


Fig. 6. Removal efficiency of Cr(III) at a concentration of 5 mg·L<sup>-1</sup> by zeolite 4A sample as a function of dose.

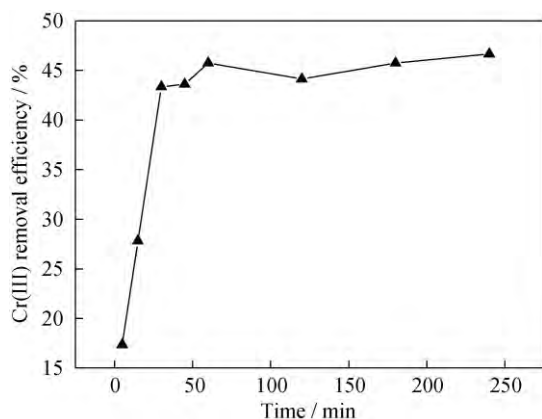
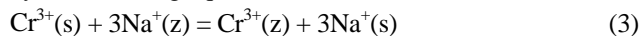


Fig. 7. Removal efficiency of Cr(III) by zeolite 4A sample at different time (temperature, 25°C; pH 4; Cr(III) initial concentration, 100 mg·L<sup>-1</sup>; volume, 100 mL).

### 3.3.5. Mechanism of the removal of Cr(III) by zeolite 4A

It is well known that zeolite 4A has a high ion-exchange capacity for a variety of cations. It can be found in the literature [8,28,30] that the main mechanism of the removal of Cr(III) by zeolite 4A is ion exchange. This can be explained by the following equation:



where (s) and (z) indicate the solution and zeolite 4A, respectively.

Fig. 8 shows the XRD pattern of the solid product obtained after the Cr(III) removal reaction. It was found that the characteristic peaks of zeolite 4A disappeared and two new characteristic peaks appeared. These peaks could be identified by XRD. From this analysis it was deduced that the reactants Cr(III) and zeolite 4A were transformed into the products Cr<sub>2</sub>(OH)<sub>6</sub>(H<sub>2</sub>O)<sub>4</sub>·2H<sub>2</sub>O and Na<sub>8</sub>(AlSiO<sub>4</sub>)<sub>6</sub>(OH)<sub>2</sub>·4H<sub>2</sub>O, respectively. It is known that the crystal structure of zeolite

4A may be damaged during exchange of an excess of Na<sup>+</sup> by other cations such as Fe<sup>2+</sup>, Co<sup>2+</sup>, Ni<sup>2+</sup>, and Cu<sup>2+</sup> [31]. Therefore, the disappearance of zeolite 4A and the appearance of Na<sub>8</sub>(AlSiO<sub>4</sub>)<sub>6</sub>(OH)<sub>2</sub>·4H<sub>2</sub>O indicated that the crystal structure of zeolite 4A was damaged and that the ion-exchange reaction occurred in the removal process. However, the formation of Cr<sub>2</sub>(OH)<sub>6</sub>(H<sub>2</sub>O)<sub>4</sub>·2H<sub>2</sub>O was not consistent with the ion-exchange principle shown in Eq. (3). Thus, it was surmised that a different removal mechanism simultaneously existed during the removal process.

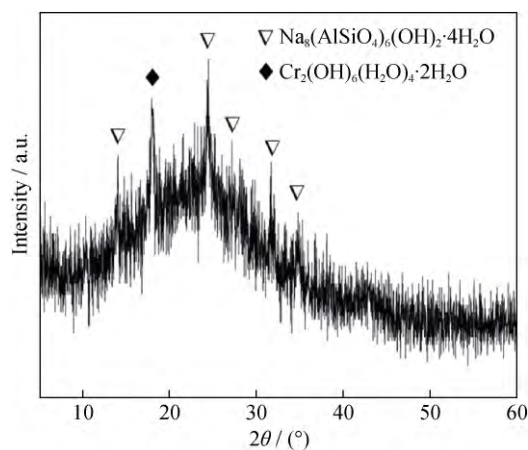
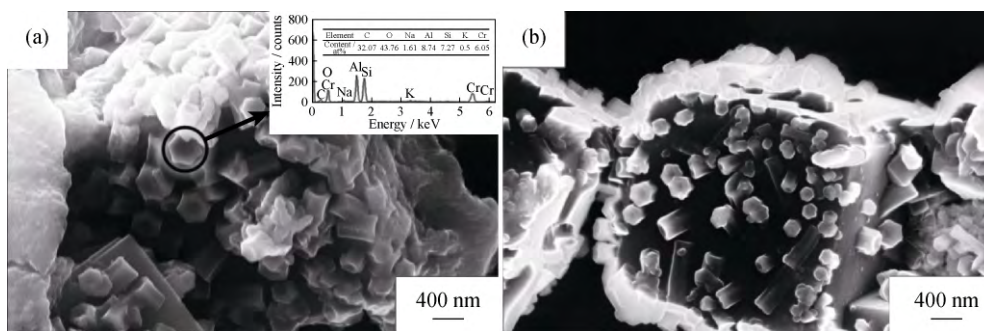


Fig. 8. XRD pattern of the solid product obtained after the Cr(III) removal reaction.

Fig. 9 shows SEM images of the solid products obtained after removing the Cr(III) ions at different initial concentrations of Cr(III) in the solution. It can be clearly seen that new rod-shaped crystals formed on the surface of the crystal particles of zeolite 4A. The EDS results of these crystals, marked by the circle, indicate that some Cr(III) ions in the solution are transformed to the new rod-shaped crystals during the removal process. Meanwhile, by combining these results with the analysis results of the XRD pattern in Fig. 8, it was concluded that the rod-shaped crystal is Cr<sub>2</sub>(OH)<sub>6</sub>(H<sub>2</sub>O)<sub>4</sub>·2H<sub>2</sub>O. Hence, the mechanism involved could be deduced as follows. Firstly, the Cr(III) cations around zeolite 4A were attracted to the surface of the zeolite 4A particles by electrostatic forces. Then they were connected to the TO<sub>4</sub> (T refers to Al or Si) tetrahedron structure by replacing the hydrogen in the hydroxyl group. As more and more Cr(III) ions became attached to each other on the surface of zeolite 4A, they generated new crystal seeds. Finally, these new crystal seeds grew on the surface of the crystal particles and formed the new crystal Cr<sub>2</sub>(OH)<sub>6</sub>(H<sub>2</sub>O)<sub>4</sub>·2H<sub>2</sub>O. Thus, from all the present results, it was concluded that the mechanism in this case was surface adsorption–crystallization.



**Fig. 9.** SEM images of samples obtained after the removal reaction of Cr(III) by zeolite 4A. The initial Cr(III) concentrations of (a) and (b) are  $100 \text{ mg}\cdot\text{L}^{-1}$  and  $5 \text{ mg}\cdot\text{L}^{-1}$ , respectively.

The above two mechanisms did not remove Cr(III) separately. They are most likely to be interrelated with each other. As shown in Fig. 9, two different solid products were obtained after the removal reaction of Cr(III) by zeolite 4A. By comparing the two images, it was found that the population of the new rod-shaped crystals formed on the surface of zeolite 4A in the solution with a Cr(III) concentration of  $100 \text{ mg}\cdot\text{L}^{-1}$  (Fig. 9(a)) was much greater than that in Fig. 9(b) with a Cr(III) concentration of  $5 \text{ mg}\cdot\text{L}^{-1}$ . On the other hand, Fig. 5 shows that the Cr(III) removal capacity by zeolite 4A at a concentration of  $100 \text{ mg}\cdot\text{L}^{-1}$  was lower than that at a concentration of  $5 \text{ mg}\cdot\text{L}^{-1}$ . It is interesting to note that the number of rod-shaped crystals decreased while the removal capacity increased, and *vice versa*. This could be attributed to the fact that the new rod-shaped crystals formed on the surface of the zeolite 4A particles might block the nanopores inside the particles of zeolite 4A, thereby hindering the outward diffusion of chromium and the inward diffusion of sodium cations in the solution. This would further decrease the Cr(III) exchange capacity of zeolite 4A and thus decrease the removal capacity of Cr(III) by zeolite 4A. Thus, the greater the number of rod-shaped crystals present, the lesser the Cr(III) exchange capacity of zeolite 4A.

The removal of Cr(III) by zeolite 4A was a complex process in which both the ion-exchange process and the surface adsorption–crystallization process played significant roles. The two processes were interrelated and mutually restrictive, and also promoted each other. In combination, a complete removal of Cr(III) from solution could be achieved.

#### 4. Conclusions

(1) The present study shows that a single phase zeolite 4A sample with high performance can be synthesized from bauxite tailings by an improved method, impurity Fe has been removed without HCl leaching, which is more

cost-effective and environmentally friendly. It is shown that the zeolite 4A sample obtained is of high purity and is crystalline. The synthesized crystal has a cubic structure with chamfered edges, and the particle size is much smaller than that obtained in the previous work.

(2) The new zeolite 4A shows high removal capacity for Cr(III), especially in solutions with lower initial concentrations of Cr(III). The removal capacity of Cr(III) by zeolite 4A is affected by the initial pH value of the solution and reaches the maximum value at a pH value of 4. The removal capacity is also affected by the initial concentration of Cr(III) ( $5$  to  $100 \text{ mg}\cdot\text{L}^{-1}$ ) in the solution and decreases with increasing Cr(III) concentration. The maximum removal capacity was found to be  $85.1 \text{ mg}\cdot\text{g}^{-1}$ , measured at the initial pH value of 4 and the initial Cr(III) concentration of  $5 \text{ mg}\cdot\text{L}^{-1}$ . The results indicate that at low concentrations of Cr(III) in the solution, the removal of Cr(III) by zeolite 4A can compensate for the shortcomings of the chemical precipitation method.

(3) Kinetic investigation shows that Cr(III) removal occurred quickly, in 30 min. An important conclusion from the present results is that the removal of Cr(III) by zeolite 4A is not only caused by an ion-exchange process, but is also due to a surface adsorption–crystallization process.

#### Acknowledgements

This work was financially supported by the National High Technology Research and Development Program of China (No. 2013AA032003) and the National Natural Science Foundation of China (Nos. 51372019, 51272025, and 51072022).

#### References

- [1] S.E. Fendorf, Surface reactions of chromium in soils and waters, *Geoderma*, 67(1995) No. 1-2, p. 55.
- [2] I.J. Buerge and S.J. Hug, Influence of mineral surfaces on

- chromium(VI) reduction by iron(II), *Environ. Sci. Technol.*, 33(1999), No. 23, p. 4285.
- [3] T. Hu and Y.Y. Li, Advance in Cr-containing wastewater treatments, *Pollut. Control Technol.*, 18(2005), No. 4, p. 5.
- [4] D.J. Wang and X.Y. He, Progress of the chromic wastewater treatment processes, *Anhui Chem. Ind.*, 33(2007), No. 1, p. 12.
- [5] H.Q. Zhang, K.G. Zhou, and Y.D. Wu, Removal of Cr<sup>6+</sup> and Mn<sup>2+</sup> from electrolytic manganese wastewater, *Nonferrous Met. Sci. Eng.*, 5(2014), No. 3, p. 9.
- [6] N.B. Guo, M.C. Jia, and X.T. Dong, Treatment of chromium-containing radioactive wastewater by redox-precipitation-ultrafiltration method, *J. Wuhan Univ. Technol. Transp. Sci. Eng.*, 37(2013), No. 1, p. 196.
- [7] E. Erdem, N. Karapinar, and R. Donat, The removal of heavy metal cations by natural zeolites, *J. Colloid Interface Sci.*, 280(2004), No. 2, p. 309.
- [8] S.B. Wang and Y.L. Peng, Natural zeolites as effective adsorbents in water and wastewater treatment, *Chem. Eng. J.*, 156(2010), No. 1, p. 11.
- [9] S.F. Mousavi, M. Jafari, M. Kazemimoghdam, and T. Mohammadi, Template free crystallization of zeolite Rho via hydrothermal synthesis: effects of synthesis time, synthesis temperature, water content and alkalinity, *Ceram. Int.*, 39(2013), No. 6, p. 7149.
- [10] F. Hasan, R. Singh, G. Li, D.Y. Zhao, and P.A. Webley, Direct synthesis of hierarchical LTA zeolite via a low crystallization and growth rate technique in presence of cetyltrimethylammonium bromide, *J. Colloid Interface Sci.*, 382(2012), No. 1, p. 1.
- [11] C. Kosanović, B. Subotić, and A. Ristić, Kinetic analysis of temperature-induced transformation of zeolite 4A to low-carnegeite, *Mater. Chem. Phys.*, 86(2004), No. 2-3, p. 390.
- [12] C.O. Arean, G.T. Palomino, M.R.L. Carayol, A. Pulido, M. Rubeš, O. Bludský, and P. Nachtigall, Hydrogen adsorption on the zeolite Ca-A: DFT and FT-IR investigation, *Chem. Phys. Lett.*, 477(2009), No. 1-3, p. 139.
- [13] L. Damjanović, V. Rakić, V. Rac, D. Stošić, and A. Auroux, The investigation of phenol removal from aqueous solutions by zeolites as solid adsorbents, *J. Hazard. Mater.*, 184(2010), No. 1-3, p.477.
- [14] I.A. Khan and K.F. Loughlin, Kinetics of sorption in deactivated zeolite crystal adsorbents, *Comput. Chem. Eng.*, 27(2003), No. 5, p. 689.
- [15] A. Baldansuren, R.A. Eichel, and E. Roduner, Nitrogen oxide reaction with six-atom silver clusters supported on LTA zeolite, *Phys. Chem. Chem. Phys.*, 11(2009), No. 31, p. 6664.
- [16] H.S. Sherry and H.F. Walton, The ion-exchange properties of zeolites. II. Ion exchange in the synthetic zeolite Linde 4A, *J. Phys. Chem.*, 71(1967), No. 5, p. 1457.
- [17] M.W. Ackley, S.U. Rege, and H. Saxena, Application of natural zeolites in the purification and separation of gases, *Microporous Mesoporous Mater.*, 61(2003), No. 1-3, p. 25.
- [18] P. Varelziz, E.S. Kikkinides, and M.C. Georgiadis, On the optimization of gas separation processes using zeolite membranes, *Chem. Eng. Res. Des.*, 81(2003), No. 5, p. 525.
- [19] T. Du, L.Y. Liu, P. Xiao, S. Che, and H.M. wang, Preparation of zeolite NaA for CO<sub>2</sub> capture from nickel laterite residue, *Int. J. Miner. Metall. Mater.*, 21(2014), No. 8, p. 820.
- [20] S. Aguado, G. Bergeret, C. Daniel, and D. Farrusseng, Absolute molecular sieve separation of ethylene/ethane mixtures with silver zeolite A, *J. Am. Chem. Soc.*, 134(2012), No. 36, p. 14635.
- [21] K.S. Hui and C.Y.H. Chao, Pure, single phase, high crystalline, chamfered-edge zeolite 4A synthesized from coal fly ash for use as a builder in detergents, *J. Hazard. Mater.*, 137(2006), No. 1, p. 401.
- [22] H. Upadek, E. Smulders, and J. Poethkow, Laundry detergent additive containing zeolite, polycarboxylate, and perborate, *Zeolites*, 11(1991), No. 1, p. 90.
- [23] C. Covarrubias, R. Arriagada, J. Yáñez, R. García, M. Angélica, S.D. Barros, P. Arroyo, and E.F. Sousa-Aguiar, Removal of chromium(III) from tannery effluents, using a system of packed columns of zeolite and activated carbon, *J. Chem. Technol. Biotechnol.*, 80(2005), No. 8, p. 899.
- [24] Q.H. Lu and Y.H. Hu, Synthesis of aluminum tri-polyphosphate anticorrosion pigment from bauxite tailings, *Trans. Nonferrous Met. Soc. China*, 22(2012), No. 22, p. 483.
- [25] D.Y. Ma, Z.D. Wang, M. Guo, M. Zhang, and J.B. Liu, Feasible conversion of solid waste bauxite tailings into highly crystalline 4A zeolite with valuable application, *Waste Manage*, 34(2014), No. 11, p.2365.
- [26] C. Lao-Luque, M. Solé, X. Gamisans, C. Valderrama, and A.D. Dorado, Characterization of chromium(III) removal from aqueous solutions by an immature coal (leonardite). Toward a better understanding of the phenomena involved, *Clean Technol. Environ. Policy*, 16(2014), No. 1, p. 127.
- [27] D. Rai, B.M. Sass, and D.A. Moore, Chromium(III) hydrolysis constants and solubility of chromium(III) hydroxide, *Inorg. Chem.*, 26(1987), No. 3, p. 345.
- [28] K.S. Hui, C.Y.H. Chao, and S.C. Kot, Removal of mixed heavy metal ions in wastewater by zeolite 4A and residual products from recycled coal fly ash, *J. Hazard. Mater.*, 127(2005), No. 1-3, p.89.
- [29] American Public Health Association (APHA), *Standard Methods for the Examination of Water and Wastewater*, Washington, D.C., 1995.
- [30] I.J. Gal, O. Janković, S. Malčić, P. Radovanov, and M. Todorović, Ion-exchange equilibria of synthetic 4A zeolite with Ni<sup>2+</sup>, Co<sup>2+</sup>, Cd<sup>2+</sup> and Zn<sup>2+</sup> ions, *Trans. Faraday Soc.*, 67(1971), p. 999.
- [31] N.H. Heo, W. Cruz-Patalinghug, and K. Seff, Crystal structure of zeolite 4A ion exchanged to the limit of its stability with nickel(II), *J. Phys. Chem.*, 90(1986), No. 17, p. 3931.